BIOORGANIC CHEMISTRY 17, 64–78 (1989)

Non-Steady-State Kinetics for the Carboxypeptidase A-Catalyzed Hydrolysis of *O*-[*trans*-(α-Benzoylamino)cinnamoyl]-L-mandelate: Evidence for the Productive Nature of the Accumulating Intermediate

JUNGHUN SUH,[1] SHIN CHUNG, AND GIL BAE CHOI

Department of Chemistry, Seoul National University, Seoul 151-742, Korea

Received April 5, 1988

The carboxypeptidase A-catalyzed hydrolysis of *O*-[*trans*-(α-benzoylaminocinnamoyl)]-L-mandelate was kinetically investigated under the condition of either $S_o \gg E_o$ or $S_o < E_o$ at −4.1°C and pH 7.5. Analysis of the data obtained under both conditions revealed that an intermediate (ES′) other than the Michaelis complex (ES) should accumulate in significant concentrations compared with S_o when $S_o < E_o$. The absorbance changes observed when $S_o < E_o$ were analyzed with non-steady-state rate expressions by assuming that the accumulating intermediate ES′ is the product of a side equilibrium unrelated to the main reaction path. The values of kinetic parameters thus calculated, however, indicate that ES should be preferentially converted into the products instead of ES′. Thus, ES′ cannot accumulate if the reaction proceeds through this mechanism. On the other hand, analysis of the non-steady-state kinetic data on the basis of the productive nature of ES′ showed that ES′ accumulates under the present conditions. Therefore, the non-steady-state kinetic data indicated that the accumulating intermediate is present on the main reaction path instead of a side equilibrium. The possible structure of ES′ of the present reaction is discussed in the light of previously reported kinetic and trapping experiments.

In the mechanistic studies of carboxypeptidase A (CPA)[2] (EC 3.4.17.1), the most controversial issue has been whether the Glu-270 carboxylate acts as a general base or as a nucleophile (*1–19*).

During the CPA-catalyzed hydrolysis of *O*-[*trans*-(α-acylaminocinnamoyl)]-L-β-phenyllactate (**1a, 1b**), accumulation of stable intermediates in near quantitative yields was observed at −2°C spectrophotometrically (*4*). The first-order rate constant for the breakdown of the intermediate was identical with k_{cat}. The k_{cat} value was almost the same for **1a** and *O*-[*trans*-(α-benzoylaminocinnamoyl)]-L-mandelate **(2)** and was independent of pH for both **1a** and **2** (*4, 5*). In addition, the $K_m$app values for **1a, 1b,** or **2** were much smaller compared with other L-β-phenyllactate or L-mandelate ester substrates. The results obtained with **1a, 1b,** and **2** were explained in terms of the nucleophilic mechanism, assuming that the accumulating intermediate is the anhydride formed between the acyl portion of the substrate and the Glu-270 carboxylate of CPA (*4, 5*).

[1] To whom correspondence should be addressed.

[2] Abbreviation used: CPA, carboxypeptidase A.

0045-2068/89 $3.00

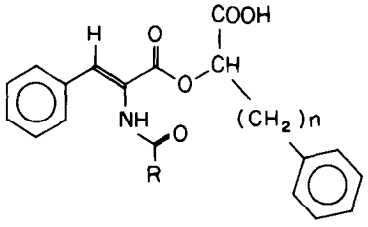

1a: R = phenyl, $n = 1$
1b: R = 2-naphthyl, $n = 1$
2: R = phenyl, $n = 0$.

In the determination of mechanisms of chemical reactions, identification of intermediates plays a key role. Even if an intermediate accumulates and is detected in a reaction mixture or isolated from it, however, this is not conclusive proof that it is a true intermediate lying on the path from reactants to products. It could well arise from a side-equilibrium, unrelated to the main reaction (*20*).

In uni-substrate enzymatic reactions, accumulating intermediate ES′ in Scheme I represents a productive intermediate, while that in Scheme II stands for a side-equilibrium product.[3-5]

Scheme I

$$E + S \underset{k_{-1}}{\overset{k_1}{\rightleftharpoons}} ES \underset{k_{-2}}{\overset{k_2}{\rightleftharpoons}} ES' \xrightarrow{k_3} E + P_i$$

[3] The following schemes may be regarded as alternative forms of Scheme II:

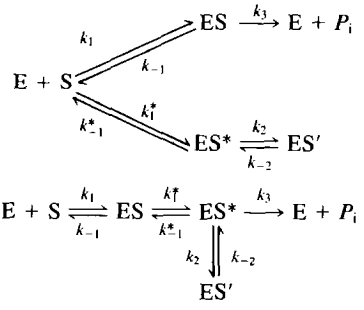

If ES and ES* are in rapid equilibria with E and S,[4] these schemes are kinetically identical with Scheme II. Alternatively, complexes (e.g., EP_1P_2) formed between the enzyme and the products may exist on the reaction course of transformation of ES′ (Scheme I) or ES (Scheme II) into the product. However, it is easy to judge whether such complexes can accumulate under the experimental conditions. When such complexes do not accumulate in significant amounts as in the reaction of CPA presented in this article, it is not necessary to include such complexes in the reaction scheme.

[4] In the study of the pre-steady-state kinetics under the conditions of $S_o \gg E_o$ for the CPA-catalyzed hydrolysis of dansyl-containing ester and peptide substrates using spectrofluorometry at sub-zero temperatures (*14*), it was established that the equilibrium between S, E, and ES is reached within the mixing period of the stopped-flow apparatus (*14*). When analyzed according to Scheme I, the pre-steady-state kinetic data indicated the presence of the k_{-2} step. Analysis of the pre-steady-state kinetic data for the formation and breakdown of ES′ led to the values of K_s ($= k_{-1}/k_1$), k_2, k_{-2}, and k_3 of Scheme I. The kinetic data are, however, also compatible with Scheme II. The pre-steady-state kinetic data, therefore, cannot differentiate Scheme I and Scheme II.

[5] The peculiar behavior manifested by the steady-state kinetic data for the CPA-catalyzed hydrolysis of **1a, 1b,** and **2** which have been explained (*4, 5*) in terms of Scheme I may be also accounted for with Scheme II by making some necessary assumptions.

Scheme II

$$E + S \underset{k_{-1}}{\overset{k_1}{\rightleftharpoons}} ES \xrightarrow{k_3} E + P_i.$$
$$\qquad\qquad\quad k_2 \Big\downarrow \Big\uparrow k_{-2}$$
$$\qquad\qquad\quad ES'$$

In the CPA-catalyzed reactions or in any other chemical reaction in general, the accumulating intermediate does not provide any decisive information on the mechanism of the main reaction path, unless it is clarified that the intermediate is a productive one. In the present study, non-steady-state kinetics[6] of the CPA-catalyzed hydrolysis of **2** are investigated. As is presented in this article, the kinetic data are compatible with Scheme I, but are inconsistent with Scheme II. The present results, therefore, reveal that the accumulating intermediate is a productive one.

EXPERIMENTAL PROCEDURES

Materials. Substrate **2** was prepared as described previously (*5*). Carboxypeptidase A_γ was purchased as a suspension in toluene/water from Worthington (Cooper Biomedical). Preparation of the stock solutions and the assay of the enzyme activity were performed as reported previously (*4*).

Kinetic measurements. Reaction rates were measured with a Beckman 5260 UV/Vis spectrophotometer by following the absorbance changes at 310 nm. At this wavelength, CPA ($<2 \times 10^{-4}$ M) and L-β-phenyllactate ($<3 \times 10^{-4}$ M) do not absorb and the absorbance changes observed during the CPA-catalyzed reaction of **2** are attributable to the substrate, the enzyme–substrate complexes, and *trans*-(α-benzoylamino)cinnamate. The extinction coefficient of **2** at 310 nm was greater than that of *trans*-(α-benzoylamino)cinnamate by about 4500 M^{-1} cm^{-1} under the experimental conditions. When S_o, the initially added concentration of **2**, was $\geq 2.9 \times 10^{-5}$ M (Table 1), the reaction rates were followed by using cuvettes with a 1-cm light path. When S_o was 0.61×10^{-5} M, however, a specially designed cuvette with a 4-cm light path was employed. Temperature was controlled at -4.1 ± 0.2°C with a Lauda Brinkman T-2 circulator. The pH of the reaction mixtures was adjusted at 7.50 with 0.05 M *N*-2-hydroxyethylpiperazine-*N'*-2-ethanesulfonic acid, and the ionic strength maintained at 1.0 M with sodium chloride. pH measurements were carried out with a Dongwoo DP-215 pH meter.

RESULTS

The steady-state kinetics of the CPA-catalyzed hydrolysis of **2** were measured at −4.1°C under the condition of $S_o \gg E_o$ (S_o; $0.4 \sim 3 \times 10^{-4}$ M, E_o (total enzyme concentration); 1.45×10^{-6} M), as described previously (*4*). From the linear plot

[6] The term "non-steady-state kinetics" refers to the systems in which the kinetic data cannot be analyzed either by the pre-steady-state rate expressions or by the steady-state rate expressions.

TABLE 1

Conditions of the Non-Steady-State Kinetic Measurements for the CPA-Catalyzed Hydrolysis of **2** and the Values of the Pseudo-First-Order Rate Constants

E_o (10^{-5} M)	E_m[a] (10^{-5} M)	S_o (10^{-5} M)	k_o (10^{-3} s_{-1})
17.6	16.3 (16.6)	5.15	14.5
13.5	12.5 (12.7)	4.64	11.4
10.5	9.73 (9.88)	4.06	9.28
8.20	7.63 (7.73)	3.48	6.66
7.03	6.57 (6.66)	3.09	6.49
5.88	5.80 (5.81)	0.61	4.99
5.86	5.48 (5.54)	2.90	5.60
3.92	3.86 (3.87)	0.61	3.21
2.94	2.89 (2.90)	0.61	2.57
1.96	1.93 (1.93)	0.61	1.51
0.98	0.96 (0.96)	0.61	0.91

[a] The values indicated outside the parentheses were calculated as mentioned in footnote 7. The values in parentheses were obtained as $E_m = (E_o - [ES']_{max}/2)$ for which $[ES']_{max}$, the maximum concentration of ES' accumulating during the reaction, was calculated by using the values of F and G estimated from the non-steady-state kinetic data shown under Discussion and in Fig. 5.

of E_o/v_o vs $1/S_o$ which is illustrated in Fig. 1, the k_{cat} value of $(1.32 \pm 0.07) \times 10^{-2}$ s^{-1} and the $K_m$app value of $(1.54 \pm 0.09) \times 10^{-4}$ M were obtained.

The absorbance changes at 310 nm were also measured under the conditions of $S_o < E_o$ at -4.1°C. The values of E_o and S_o for each run are listed in Table 1. The absorbance change of a typical reaction is illustrated in Fig. 2. The plots of log Abs against time (t) (Abs; absorbance value at each t minus that at $t = \infty$) were linear for at least two half-lives in the reactions measured under the conditions of $S_o < E_o$, and the pseudo-first-order rate constants (k_o) were calculated from the logarithmic plots.

For the simple Michaelis-Menten scheme of Eq. [1], pseudo-first-order reactions are observed under the conditions of $[E] \approx E_o$ when steady states are attained and the corresponding pseudo-first-order rate constants are represented by Eq. [2]. The linear transform of Eq. [2] is Eq. [3]:

$$E + S \underset{K_m\text{app}}{\rightleftharpoons} ES \xrightarrow{k_{cat}} E + P_i \qquad [1]$$

$$k_o = k_{cat}[E]/\{K_m\text{app} + [E]\} \qquad [2]$$

$$1/k_o = (K_m\text{app}/k_{cat})(1/[E]) + 1/k_{cat}. \qquad [3]$$

The value of [E] can be maintained constant at E_o during the reaction if $E_o \gg S_o$. However, the spectral property of **2** did not allow kinetic measurements at very

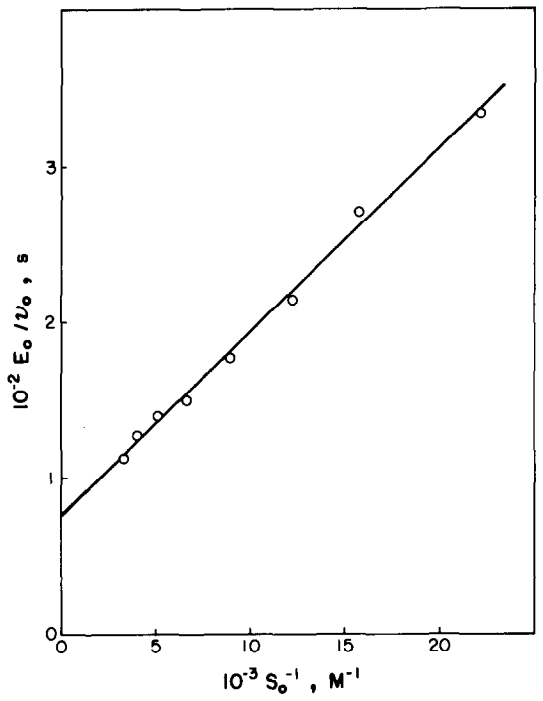

FIG. 1. Plot of E_o/v_o against $1/S_o$ for the CPA-catalyzed hydrolysis of **2** under the conditions of $S_o \gg E_o$.

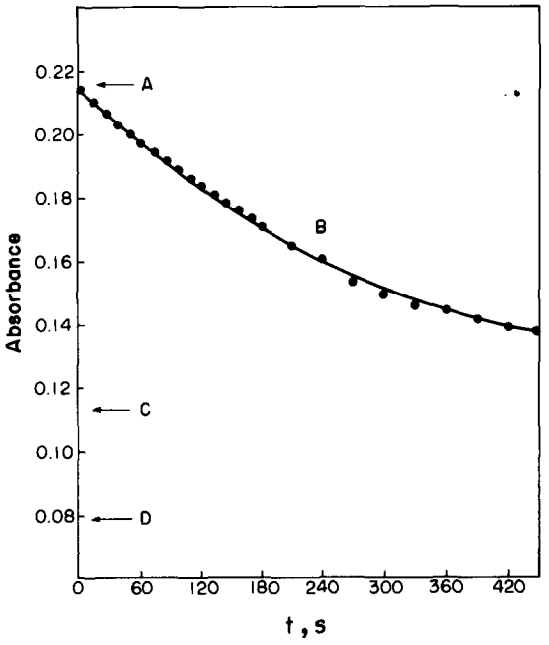

FIG. 2. Absorbance readings at 310 nm and −4.1°C (light path; 4 cm). (A) The absorbance observed for **1a** and **2** ($S_o = 0.61 \times 10^{-5}$ M) in the absence of CPA; (B) the absorbance change observed after mixing **2** ($S_o = 0.61 \times 10^{-5}$ M) with CPA ($E_o = 3.92 \times 10^{-5}$ M) (the solid line represents the data fitting according to pseudo-first-order kinetics); (D) the absorbance observed immediately after mixing **1a** ($S_o = 0.61 \times 10^{-5}$ M) with CPA ($E_o = 3.92 \times 10^{-5}$ M); (C) the absorbance of the hydrolysis products for **1a** or **2** ($[P_i] = 0.61 \times 10^{-5}$ M).

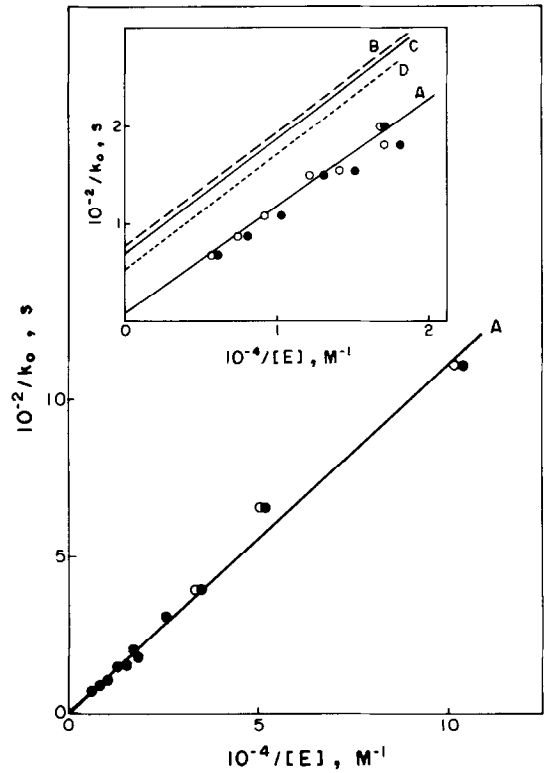

FIG. 3. Plot of $1/k_o$ against 1/[E] for the CPA-catalyzed hydrolysis of **2** under the conditions of $S_o < E_o$, (●, data points obtained by using $[E]_m$ as [E]; ○, those obtained by using E_o as [E]). Line A represents the line obtained by the linear regression of data points, ●. Line B is the hypothetical line constructed by assuming that the reaction proceeds through the mechanism of Eq. [1] and by using the k_{cat} and $K_m$app values obtained from the steady-state kinetic data. Lines C and D are the hypothetical lines constructed by assuming that the mechanism of Scheme II is operative and by using the k_2/k_3 values of 0.3 and 0.2, respectively, as indicated under Discussion.

small S_o concentrations. The upper limits ($[EX]_{max}$) for the concentrations of the enzyme species containing substrate or products was calculated by using the observed value of $K_m$app.[7] The median value (E_m) of [E] obtained by correcting E_o with this upper limit concentration ($E_m = E_o - [EX]_{max}/2$) are indicated in Table I for each run measured under the conditions of $S_o < E_o$. Comparison of E_m and E_o indicates that [E] is kept at E_m within $\pm 2 \sim 6\%$ during the courses of the reaction under the present conditions.

The values of $1/k_o$ measured under the conditions of $S_o < E_o$ for the CPA-catalyzed hydrolysis of **2** are plotted against 1/[E] in Fig. 3. Line B of Fig. 3 represents the theoretical line constructed according to Eq. [3] by using the k_{cat} and $K_m$app values which were obtained from the steady-state kinetic data mea-

[7] The maximum amount of ([ES] + [ES']) is calculated by assuming that ES' as well as ES reach steady states immediately after mixing **2** with CPA. Binding of L-mandelate (K_p = ca. 2 mM) (*9*) can be ignored under the present conditions.

sured under the conditions of $S_o \gg E_o$. The values of k_{cat} and $K_m$app calculated from line A of Fig. 3 according to Eq. [3] are about 10 times greater than the values of k_{cat} and $K_m$app calculated from the steady-state kinetic data. The absorbance changes measured under the conditions of $S_o < E_o$, therefore, do not represent steady-state kinetics.

Since it is highly unlikely that the formation of the ES complex does not reach equilibrium or a steady state within several minutes,[4] the simple Michaelis-Menten scheme of Eq. [1] does not adequately describe the reaction. Instead, the analysis of the kinetic data measured for the CPA-catalyzed hydrolysis of **2** under the conditions of $S_o < E_o$ requires the presence of the ES′ complex as in Schemes I and II. In addition, the formation of ES′ is not to reach a steady state for the CPA-catalyzed hydrolysis of **2** under the present conditions of $E_o > S_o$. If a steady-state is attained for ES′ of Scheme I or Scheme II, the kinetic data should obey Eq. [3] for which k_{cat} and $K_m$app are expressed by the equations summarized in Table 2. Furthermore, ES′ must accumulate in significant concentrations in comparison with S_o during the course of the reaction in order for the absorbance change to manifest noticeably anomalous behavior.

TABLE 2

Expressions of k_{cat} and $K_m$app for Schemes I and II

Scheme	Parameter	Expression	Condition	Eq. No.
I	k_{cat}	$k_2k_3/(k_2 + k_3 + k_{-2})$		[4]
	k_{cat}	k_3	$k_2 \gg (k_3 + k_{-2})^a$	[5]
	$K_m$app	$\dfrac{(k_2k_3 + k_{-1}k_3 + k_{-1}k_{-2})}{k_1(k_2 + k_3 + k_{-2})}$		[6]
	$K_m$app	$\dfrac{K_mk_3}{k_2} + \dfrac{k_{-1}k_{-2}}{k_1k_2}$ $\ll K_m = \dfrac{k_{-1} + k_2}{k_1}$	$k_2 \gg (k_3 + k_{-2})^a$	[7]
	$K_m$app	$K_s(k_3 + k_{-2})/k_2$ $\ll K_s = k_{-1}/k_1$	$k_2 \gg (k_3 + k_{-2})^a$ and $k_{-1} \gg k_2^b$	[8]
II	k_{cat}	$k_3/(1 + k_2/k_{-2})$		[9]
	k_{cat}	k_3k_{-2}/k_2	$k_2 \gg k_{-2}^a$	[10]
	$K_m$app	$\dfrac{(k_{-1} + k_3)}{k_1(1 + k_2/k_{-2})}$ $= K_m/(1 + k_2/k_{-2})$ where K_m is $(k_{-1} + k_3)/k_1$		[11]
	$K_m$app	K_mk_{-2}/k_2	$k_2 \gg k_{-2}^a$	[12]
	$K_m$app	K_sk_{-2}/k_2 where $K_s = k_{-1}/k_1$	$k_2 \gg k_{-2}^a$ and $k_{-1} \gg k_3^b$	[13]

[a] For ES′ to accumulate, [ES′] $\gg$ [ES] at a steady state, since [ES] is negligible compared with S_o in the CPA-catalyzed hydrolysis of **2** under usual experimental conditions. Then, $k_2 \gg (k_3 + k_{-2})$ for Scheme I and $k_2 \gg k_{-2}$ for Scheme II.

[b] See footnote 4. When rapid equilibrium is attained among E, S, and ES, $K_s = K_m$. In the case of the rapid equilibration, $k_{-1} \gg k_2$ for Scheme I and $k_{-1} \gg (k_2 + k_3)$ for Scheme II.

TABLE 3

Expressions of Non-Steady-State Kinetic Parameters and Their Relationship with Steady-State Kinetic Parameters for Schemes I and II

Parameter	Scheme	Expression
A	I, II	$\{G + (G^2 - 4F)^{1/2}\}/2$
B	I, II	$\{G - (G^2 - 4F)^{1/2}\}/2$
C	I, II	$(k_2/K_s)S_o[E]/(B - A)(1 + [E]/K_s)$
D	I	$k_{-2} + k_3$
	II	k_{-2}
F[a]	I, II	$I[E]/(1 + [E]/K_s)$
G[b]	I, II	$J[E]/(1 + [E]/K_s) + D$
I	I	k_2k_3/K_s
	II	$k_{-2}k_3/K_s$
J	I	k_2/K_s
	II	$(k_3 + k_2)/K_s$
k_{cat}	I	I/J[c]
	II	$I/(J - I/D)$[c]
$K_m$app	I	D/J[c]
	II	$D/(J - I/D)$[c]
k_{cat}/K_mapp	I, II	I/D[c]

[a] F is $(A \times B)$.

[b] G is $(A + B)$.

[c] Derived under the conditions of $k_2 \gg (k_3 + k_{-2})$ and $k_{-1} \gg k_2$ for Scheme I and those of $k_2 \gg k_{-2}$ and $k_{-1} \gg k_3$ for Scheme II. See footnotes of Table 2.

The non-steady-state expressions of [S], [ES], and [ES′] for Schemes I and II are Eqs. [14]–[16] which are derived as indicated in Appendix. The expressions of A, B, C, and D contained in Eqs. [14]–[16] are given in Table 3.

$$[S] = (K_s/[E])(-C/k_2)\{(A - D)e^{-At} - (B - D)e^{-Bt}\} \quad [14]$$

$$[ES] = (-C/k_2)\{(A - D)e^{-At} - (B - D)e^{-Bt}\} \quad [15]$$

$$[ES'] = C(e^{-At} - e^{-Bt}). \quad [16]$$

The expression of Abs of the reaction mixture for Schemes I and II is given as Eq. [17]:

$$\begin{aligned} Abs &= \Delta\varepsilon_S[S] + \Delta\varepsilon_{ES}[ES] + \Delta\varepsilon_{ES'}[ES'] \\ &= [Abs_o/(A - B)]\{(A - H)e^{-At} - (B - H)e^{-Bt}\} \end{aligned} \quad [17]$$

$$H = D + (k_2/K_s)[E]\Delta\varepsilon_{ES'}/\{\Delta\varepsilon_S + \Delta\varepsilon_{ES}[E]/K_s\}. \quad [18]$$

Here, Abs_o is Abs at $t = 0$, and $\Delta\varepsilon_S$, $\Delta\varepsilon_{ES}$, $\Delta\varepsilon_{ES'}$, are the molar extinction coefficients of S, ES, and ES′, respectively, relative to that of P_i.

The absorbance changes observed under the conditions of $S_o < E_o$ can be analyzed in terms of Eq. [17], leading to the values of parameters Abs_o, A, B, and

H when the absorbance changes deviate significantly from pseudo-first-order kinetic behavior.[8] Then, from the dependence of F (= AB), G(= $A + B$), and H on [E] (Table 3), the values of D, I, and J are obtained. As summarized in Table 3, comparison of I/J or $I/(J - I/D)$ (estimated from the non-steady-state kinetic data) with k_{cat} (estimated from the steady-state data) and comparison of D/J or $D/(J - I/D)$ (estimated from the non-steady-state data) with $K_m$app (estimated from the steady-state data) can differentiate Scheme I from Scheme II, unless I/D is negligible compared with J.

When either $A \approx H$ or $B \approx H$,[8] Eq. [17] becomes an expression for a pseudo-first-order process with k_o representing either B or A, respectively. In this case, A, B, and H are not separately estimated, and the analysis of the non-steady-state kinetic data reveals only k_o values.

Under these conditions, F and G are related to k_o and H by Eqs. [19] and [20]:

$$k_o = AB/H = F/H \qquad [19]$$

$$k_o + H = A + B = G. \qquad [20]$$

From Eq. [19] and the definitions of H and F,

$$1/k_o = D\{1 + [E]/K_s\}/I[E] + \{1 + [E]/K_s\}L/\{1 + \Delta\varepsilon_{ES}[E]/\Delta\varepsilon_S K_s\} \qquad [21]$$

$$L = (k_2/K_s)\Delta\varepsilon_{ES'}/I\Delta\varepsilon_S. \qquad [22]$$

When $[E] \ll K_s$ and $[E] \ll K_s(\Delta\varepsilon_S/\Delta\varepsilon_{ES})$,[9] Eq. [21] becomes

$$1/k_o = (D/I)(1/[E]) + L. \qquad [23]$$

As indicated by Eq. [23], $1/k_o$ is linearly related to $1/[E]$ (Fig. 3). When E_m was taken as [E], D/I of $(1.09 \pm 0.04) \times 10^{-2}$ s M and L of 8.7 ± 15 s were obtained (*10*).

From Eq. [20] and the definitions of G and H,

$$k_o = \{J/(1 + [E]/K_s) - IL/(1 + \Delta\varepsilon_{ES}[E]/\Delta\varepsilon_S K_s)\}[E]. \qquad [24]$$

When $[E] \ll K_s$ and $[E] \ll K_s(\Delta\varepsilon_S/\Delta\varepsilon_{ES})$,[9]

$$k_o = (J - IL)[E]. \qquad [25]$$

As predicted by Eq. [25], k_o is proportional to [E] (Fig. 4). When E_m was taken as [E], $J - IL$ of 90.8 ± 2.5 s^{-1} M^{-1} was obtained and, therefore, J can be expressed as $(90.8 \pm 2.5) + (8.7 \pm 15)I$ s^{-1} M^{-1}.[10]

[8] Whether the absorbance changes deviate significantly from the pseudo-first-order behavior or not depends on the relative magnitudes of $\Delta\varepsilon_S$, $\Delta\varepsilon_{ES}$, and $\Delta\varepsilon_{ES'}$ as well as the kinetic parameters included in Schemes I and II.

[9] Considering the K_m values (*5*, *9*) of other mandelate ester substrates, K_s of **2** can be estimated as >1 mM. If the spectral properties of **2** are not altered greatly upon complexation with CPA, $\Delta\varepsilon_{ES}$ would be similar to $\Delta\varepsilon_S$. The linearity seen with the plots (Figs. 3 and 4) of k_o against [E] and $1/k_o$ against $1/[E]$ validates the assumptions of $[E] \ll K_s$ and $[E] \ll \Delta\varepsilon_S K_s/\Delta\varepsilon_{ES}$.

[10] When E_o was taken as [E], the analysis of the linear lines of Figs. 3 and 4 led to D/I of $(1.10 \pm 0.04) \times 10^{-2}$ s M, L of (14 ± 14) s, and J of $(83.1 \pm 2.1) + (14 + 14)I$ s^{-1} M^{-1}.

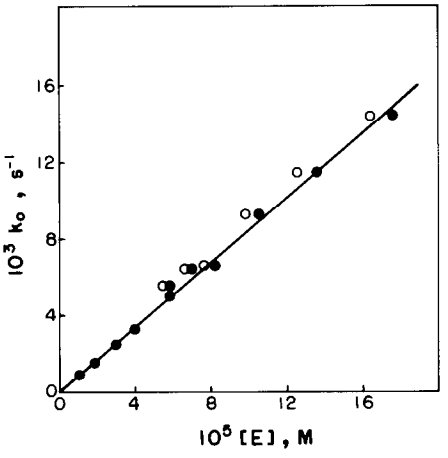

FIG. 4. Plot of k_o against [E] for the CPA-catalyzed hydrolysis of **2** under the conditions of $S_o < E_o$ (●, data points obtained by using $[E]_m$ as [E]; ○, those obtained by using E_o as [E]). The line is obtained by the linear regression of data points ●.

DISCUSSION

As indicated under Results, the anomalous absorbance changes observed for the CPA-catalyzed hydrolysis of **2** under the conditions of $S_o < E_o$ requires the existence of an additional enzyme–substrate complex (ES′), as in Schemes I and II, and its accumulation in a significant concentration during the reaction.[11]

Values of various parameters estimated from the analysis of both the steady-state and non-steady-state kinetic data in terms of Scheme I or Scheme II are summarized in Table 4. For both Scheme I and Scheme II, I/D represents k_{cat}/K_mapp. The good agreement between the value of I/D obtained from the non-steady-state kinetic data and the value of k_{cat}/K_mapp obtained from the steady-state-kinetic data indicates the validity of the analysis of the non-steady-state kinetic data presented under Results.

As summarized in Table 3, $J - I/D$ is I/k_{cat} for Scheme II. Then, $J - I/D$ is calculated as -1.0 ± 4.2 s^{-1} M^{-1} as summarized in Table 4, if Scheme II is operative.[12] Then, J (91 ± 5 s^{-1} M^{-1}) is almost identical to I/D (92 ± 3 s^{-1} M^{-1}). For Scheme II, J and I/D represent $(k_2 + k_3)/K_s$ and k_3/K_s, respectively (Table 3). Then, the results of the non-steady-state kinetic measurements indicate that $k_3 \gg$

[11] In the CPA-catalyzed hydrolysis of **1a**, the substrate is converted into ES′ right after mixing with an excess of the enzyme (Fig. 2). This is attributable to the very fast rate of the formation of ES′. In addition, ES′ accumulates quantitatively as the rate of its formation is much faster than the corresponding breakdown process.

[12] When E_o is taken as [E] in the analysis of the plot of $1/k_o$ against 1/[E] and the plot of k_o against [E], the following parameter values are obtained.[10] For Scheme II, $I/D = 91 \pm 3$ s^{-1} M^{-1} and $J = 81 \pm 6$ s^{-1} M^{-1}. For Scheme I, $D = 0.014 \pm 0.003$ s^{-1}, $I = 1.3 \pm 0.3$ s^{-2} M^{-1}, and $J = 100 \pm 20$ s^{-1} M^{-1}. Thus, essentially identical results were obtained when either E_m or E_o was used as [E] in the analysis of the non-steady-state kinetic data.

k_2 if Scheme II is operative. When $k_3 \gg k_2$, ES is converted preferentially into P_i instead of ES′, and ES′ cannot accumulate. The non-steady-state kinetic data, therefore, are not compatible with Scheme II.

For Scheme II, $I = k_{cat}(k_{cat}/K_m\text{app})(k_2/k_3)$, $J = (k_{cat}/K_m\text{app})(1 + k_2/k_3)$, and $D = k_{cat}(k_2/k_3)$. Thus, I, J, and D may be calculated for each assumed value of k_2/k_3 by using the values of k_{cat} and k_{cat}/K_mapp, if the reaction proceeds through the mechanism of Scheme II. From the slope of the plot of k_o against [E], L is expressed as $(J - 91)/I$ s. Based on the I and J values estimated for each k_2/k_3, L of 53 s is expected when $k_2/k_3 = 0.2$ and that of 69 s when $k_2/k_3 = 0.3$. By using these L values as the intercept and the D/I value (estimated as $1/(K_{cat}/K_m)$) as the slope (Eq. [23]), the plots of $1/k_o$ against 1/[E] expected when $k_2/k_3 = 0.2$ or 0.3 are illustrated in Fig. 3.[13] Thus, if Scheme II is operative, the steady-state kinetic data and the plot of k_o against [E] obtained from the non-steady-state kinetic data are to be associated with a linear line of the plot of $1/k_o$ against 1/[E] for the non-steady-state data which should be remarkably different from the observed one in order for ES′ to accumulate.

When the accumulating intermediate corresponds to ES′ of Scheme I, J is I/k_{cat} (Table 3). Then, as summarized in Table 4, the analysis of the non-steady-state kinetic data leads to $I = 1.3 \pm 0.3\ s^{-2}\ M^{-1}$ and $J = 100 \pm 20\ s^{-1}\ M^{-1}$. Consequently, from the values of I/D and k_{cat}, k_{-2} is estimated as $0.001 \pm 0.003\ s^{-1}$, being considerably smaller than k_3. The linearity observed in the plots of $1/k_o$ against 1/[E] (Fig. 3) and k_o against [E] (Fig. 4) indicates that $K_s \gg 2 \times 10^{-4}$ M. If K_s is assumed to be $>1 \times 10^{-3}$ M, k_2 ($= K_sJ$; Table 3) is estimated as $>0.1\ s^{-1}$. Thus, the analysis of the non-steady-state kinetic data in terms of Scheme I reveals $k_2 \gg (k_3 + k_{-2})$. Under these conditions, ES′ is expected to accumulate (Table 2, footnote *a*). The non-steady-state kinetic data are, therefore, compatible with Scheme I while they are inconsistent with Scheme II.

Using I, J, and D values estimated from the non-steady-state kinetic data according to Scheme I (Table 4), A, B, and C can be calculated for each [E] (Table 3).[14] Based on these values, $[ES']_{max}/S_o$ is estimated as 31% when $[E] = 1 \times 10^{-4}$ M and 20% when $[E] = 0.5 \times 10^{-4}$ M. In addition, mole fractions $[S]/S_o$, $[ES']/S_o$, and $[P]/S_o$ thus calculated are plotted against time under the conditions of $[E] = 1 \times 10^{-4}$ M and $S_o < E_o$ in Fig. 5.

[13] Based on the values of J, I, D, and k_2/K_s ($= J/(1 + k_3/k_2)$) which are calculated for each k_2/k_3 by using the k_{cat} and k_{cat}/K_mapp values obtained from the steady-state kinetic data, A, B, and C were estimated for Scheme II. With these values, $[ES']_{max}$ was estimated for each k_2/k_3. Ratio $[ES']_{max}/S_o$ thus obtained when $k_2/k_3 = 0.2$ is 8.5% for 0.5×10^{-5} M [E] and 10.7% for 1.0×10^{-4} M [E]. Therefore, even when $[ES']_{max}/S_o$ is only about 10%, the plot of $1/k_o$ against 1/[E] should be different markedly from the observed results if Scheme II is operative (Fig. 3).

[14] For Scheme I, $(H - D)$ was calculated as (11 ± 20) [E], by using the values of k_3 ($= k_{cat}$), L, and J. Then, $(H - D)$ (the second term of Eq. [18]) is estimated as $(1.1 \pm 2.0) \times 10^{-3}\ s^{-1}$ when $[E] = 1 \times 10^{-4}$ M, while D (the first term of Eq. [18]) is $(14 \pm 3) \times 10^{-3}\ s^{-1}$ regardless of [E]. Then, H does not differ appreciably from D and the second term of Eq. [18] appears to be considerably smaller than the first term. The value of B ($0.0083\ s^{-1}$ when $[E] = 1 \times 10^{-4}$ M and $0.0045\ s^{-1}$ when $[E] = 0.5 \times 10^{-4}$ M) calculated for each [E] was similar to the k_o values experimentally observed at the corresponding [E]. The calculated value of A ($0.0157\ s^{-1}$ when $[E] = 1 \times 10^{-4}$ M and $0.0145\ s^{-1}$ when $[E] = 0.5 \times 10^{-4}$ M) was very close to the estimated value of H. Thus, H is similar to A instead of B under the experimental conditions.

TABLE 4

Values of Various Kinetic Parameters Estimated by Analysis of Both the Steady-State and the Non-Steady-State Kinetic Data According to Schemes I and II[a,b]

Entry No.	Parameter	Scheme I	Scheme II	Source[c]
(1)	k_{cat} (s^{-1})	$(1.32 \pm 0.07) \times 10^{-2}$[d]		Fig. 1
(2)	$K_m$app (M)	$(1.54 \pm 0.09) \times 10^{-4}$[d]		Fig. 1
(3)	k_{cat}/K_mapp (s^{-1} M^{-1})		86 ± 5[d]	Fig. 1
(4)	I/D (s^{-1} M^{-1})		92 ± 3[d]	Fig. 3
(5)	L (s)		8.7 ± 15[d]	Fig. 3
(6)	$J - IL$ (s^{-1} M^{-1})		90.8 ± 2.5[d]	Fig. 4
(7)	J (s^{-1} M^{-1})	$(90.8 \pm 2.5) + (8.7 \pm 15)I$[d]		(5), (6)
(8)	$J - I/D$ (s^{-1} M^{-1})	$(-0.9 \pm 4.2) + (8.7 \pm 15)I$[d]		(4), (7)
(9)	I/k_{cat} (s^{-1} M^{-1})		$(76 \pm 4)I$[d]	(1)
(10)	I (s^{-2} M^{-1})	1.3 ± 0.3	-0.013 ± 0.061	(7), (9)[e] or (8), (9)[f]
(11)	J (s^{-1} M^{-1})	100 ± 20	91 ± 5	(7), (10)[g]
(12)	D (s^{-1})	0.014 ± 0.003	$(-1.4 \pm 6.6) \times 10^{-4}$	(4), (10)
(13)	k_3 (s^{-1}	0.013 ± 0.001	—	(1)
(14)	k_{-2} (s^{-1})	0.001 ± 0.003	$(-1.4 \pm 6.6) \times 10^{-4}$	(12), (13)[e] or (12)[f]
(15)	k_2 (s^{-1})	$(100 \pm 20)K_s$	—	(11)
(16)	$\Delta\varepsilon_{ES'}/\Delta\varepsilon_S$	0.11 ± 0.20	—	(1), (5)
(17)	$H - D$ (s^{-1})	(11 ± 20)[E]	—	(11), (16)
(18)	k_3/k_2	$\ll 1$	$\gg 1$	(13), (15)[e] or (4), (11)[f]

[a] Standard deviations are estimated according to the law of propagation of precision indexes (*21*). Thus, even if a parameter value is obtained by multiple stepwise calculations, the reliability of the value is reflected in its standard deviation.

[b] Non-steady-state kinetic data were analyzed by using E_m as [E].[12]

[c] The numbers in parentheses are those of the entry numbers indicated in the first column.

[d] These values are the same for Scheme I and Scheme II.

[e] For Scheme I.

[f] For Scheme II.

[g] Parameter J may be also calculated from (1) and (10) in the case of Scheme I.

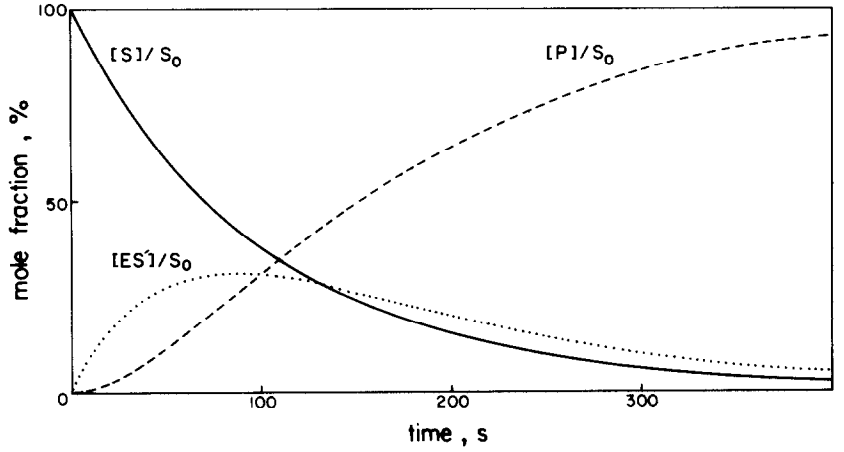

FIG. 5. Mole fractions $[S]/S_o$, $[ES']/S_o$, and $[P]/S_o$ calculated at various reaction time by using the parameter values (Table 4) estimated from the analysis of the non-steady-state kinetic data measured for the CPA-catalyzed hydrolysis of **2** in terms of the mechanism of Scheme I. Concentration $[P]$ represents that of *trans*-(α-benzoylamino)cinnamate. The calculation was performed under the conditions of E_o ($= 1 \times 10^{-4}$ M) $> S_o$.

Intermediate ES′ that accumulates during the CPA-catalyzed hydrolysis of **2** is a productive one leading to the products, and the possibility that it is the product of a side equilibrium is excluded on the basis of the non-steady-state kinetic data. This alone, of course, does not provide concrete evidence that Glu-270 acts as a nucleophile, unless the structure of the accumulating intermediate is determined.[15]

Covalent intermediates in which the acyl portions of the substrates appear to be incorporated into Glu-270 have been trapped during the CPA-catalyzed hydrolysis of *O*-(*trans*-*p*-chlorocinnamoyl)-L-β-phenyllacate, *O*-hippuryl-glycolate, or *N*-hippuryl-L-Phe at −60 or −75°C (*7, 8*).[16] Success of the trapping experiments requires the accumulation of the intermediates in significant concentrations. Although the conditions of the present study (at −4°C and in the absence of organic solvents) and the trapping experiments (at −60 or −75°C and in 50% (v/v) ethylene glycol–25% (v/v) methanol) differ greatly, it is probable that the accumulating intermediate of the present study is also a covalent acyl-CPA intermediate.[17] In addition, the pH independence of k_{cat} of **1a, 1b,** and **2** is also consistent with the accumulation of anhydride acyl-CPA intermediates as discussed previously (*4, 5*).[18]

As discussed in the introduction the detection, isolation, and characterization of intermediates play a key role in the determination of mechanisms of chemical reactions in general. Even when the presence of an intermediate is proved, however, it remains to be resolved whether it is a productive one or a side-equilibrium product. The present study is a rare instance in which this has been achieved by utilizing non-steady-state kinetic data, and can be used as a guideline in future mechanistic studies of both enzymatic and nonenzymatic reactions.

APPENDIX

Derivation of Eqs. [14]–[16] for Scheme I. For Schemes I and II,

$$K_s = [S][E]/[ES] \qquad [A\text{-}1]$$

[15] Since **1a** and **1b** produce (*4*) very stable (in terms of both the thermodynamic and kinetic stabilities) intermediates, the structures of the intermediates may be determined by X-ray crystallography or by other physical methods.

[16] Credibility of the results of the trapping experiments, however, has been recently questioned (*22*).

[17] Isokinetic relationship was observed for the $\Delta H^{\ddagger}$ and $\Delta S^{\ddagger}$ values of k_{cat} for the CPA-catalyzed hydrolysis of **1** measured in the presence of various amounts of organic cosolvents (*6*). Thus, the addition of large amounts of organic cosolvents to the reaction media does not appear to alter the reaction mechanism.

[18] The pH independence of k_{cat} of **1a, 1b,** and **2** is also compatible with the accumulation of a tetrahedral intermediate. The tetrahedral intermediate might be formed either by the nucleophilic attack of Glu-270 or by the addition of a water molecule with the general base assistance of Glu-270. When the tetrahedral intermediate accumulates, k_{cat} represents the rate constant for its breakdown. Then, the identical k_{cat} values of **1a,** an L-β-phenyllactate ester, and **2,** a much less specific L-mandelate ester, are not easily accounted for by the accumulation of the tetrahedral intermediate. Furthermore, the thermodynamic and kinetic stability of the accumulating intermediate is hardly attributable to tetrahedral intermediates considering the instability of tetrahedral intermediates. Therefore, assignment of the accumulating species as a tetrahedral intermediate is much less reasonable than that as the anhydride intermediate.

$$S_o - [P_i] = [S] + [ES] + [ES']. \quad [A\text{-}2]$$

For Scheme I,

$$d[P_i]/dt = k_3[ES'] \quad [A\text{-}3]$$

$$d[ES']/dt = k_2[ES] - (k_{-2} + k_3)[ES']. \quad [A\text{-}4]$$

From Eqs. [A-1], [A-2], and [A-4],

$$d[ES']/dt = k_2(S_o - [P_i])/(1 + K_s/[E]) - \{k_2 + (k_{-2} + k_3)(1 + K_s/[E])\}[ES']/(1 + K_s/[E]) = a(S_o - [P_i]) - b[ES']. \quad [A\text{-}5]$$

Here, $a = k_2/(1 + K_s/[E])$ and $b = (a + k_{-2} + k_3)$, and they are constant values when [E] is maintained constant during the reaction.

From Eq. [A-5],

$$d^2[ES']/dt^2 = -ad[P_i]/dt - bd[ES']/dt. \quad [A\text{-}6]$$

From Eqs. [A-6] and [A-3],

$$d^2[ES']/dt^2 + Gd[ES']/dt + F[ES'] = 0. \quad [A\text{-}7]$$

Here, $G = b$ and $F = ak_3$. Differential Eq. [A-7] can be solved according to the method described (*23*) in the literature, leading to Eq. [16]. From Eqs. [A-4] and [16], Eq. [15] is derived. From Eqs. [A-1] and [15], Eq. [14] is obtained.

Derivation of Eqs. [14]–[16] for Scheme II. For Scheme II,

$$d[P_i]/dt = k_3[ES] \quad [A\text{-}8]$$

$$d[ES']/dt = k_2[ES] - k_{-2}[ES']. \quad [A\text{-}9]$$

From Eqs. [A-1], [A-2], and [A-9],

$$d[ES']/dt = \frac{k_2(S_o - [P_i])}{(1 + K_s/[E])} - \{k_2/(1 + K_s/[E]) + k_{-2}\}[ES'] = a(S_o - [P_i]) - b'[ES']. \quad [A\text{-}10]$$

Here, $a = k_2/(1 + K_s/[E])$ and $b' = a + k_{-2}$, and they are constant values when [E] is maintained constant during the reaction.

From Eq. [A-10],

$$d^2[ES']/dt^2 = -ad[P_i]/dt - b'd[ES']/dt. \quad [A\text{-}11]$$

From Eqs. [A-8] and [A-11],

$$d^2[ES']/dt^2 = -ak_3[ES] - b'd[ES']/dt. \quad [A\text{-}12]$$

From Eqs. [A-9] and [A-12],

$$d^2[ES']/dt^2 = -a(k_3/k_2)\{d[ES']/dt + k_{-2}[ES']\} - b'd[ES']/dt. \quad [A\text{-}13]$$

Thus, Eq. [A-7] is obtained from Eq. [A-13], although F and G are defined differently compared with Scheme I. Then, Eq. [A-7] is solved to lead to Eqs. [14]–[16] as indicated above for Scheme I.

Derivation of Eq. [17]. From the definitions of Abs, Abs_o, and K_s and from Eqs. [14]–[16], the following equations are derived.

$$\begin{aligned}\text{Abs} &= \Delta\varepsilon_S[S] + \Delta\varepsilon_{ES}[ES] + \Delta\varepsilon_{ES'}[ES'] \\ &= (\Delta\varepsilon_S + \Delta\varepsilon_{ES}[E]/K_s)[S] + \Delta\varepsilon_{ES'}[ES'] \\ &= \{(\Delta\varepsilon_S + \Delta\varepsilon_{ES}[E]/K_s)S_o/(1 + [E]/K_s)(A - B)\}\{(A - D)e^{-At} \\ &\quad - (B - D)e^{-Bt}\} - k_2S_o\Delta\varepsilon_{ES'}(e^{-At} - e^{-Bt})/(A - B)(1 + K_s/[E]) \qquad \text{[A-14]}\end{aligned}$$

$$\begin{aligned}\text{Abs}_o &= \Delta\varepsilon_S[S]_{t=0} + \Delta\varepsilon_{ES}[ES]_{t=0} \\ &= (\Delta\varepsilon_S + \Delta\varepsilon_{ES}[E]/K_s)S_o/(1 + [E]/K_s). \qquad \text{[A-15]}\end{aligned}$$

From Eqs. [A-14] and [A-15], Eq. [17] is obtained.

ACKNOWLEDGMENT

This work was supported by a grant from the Korea Science and Engineering Foundation.

REFERENCES

1. LIPSCOMB, W. N. (1974) *Tetrahedron* **30,** 1725, and references therein.
2. KAISER, E. T., AND KAISER, B. L. (1972) *Acc. Chem. Res.* **5,** 219.
3. PRINCE, R. H. (1979) *Adv. Inorg. Chem. Radiochem.* **22,** 349.
4. SUH, J., CHO, W., AND CHUNG, S. (1985) *J. Amer. Chem. Soc.* **107,** 4530.
5. SUH, J., HONG, S.-B., AND CHUNG, S. (1986) *J. Biol. Chem.* **261,** 7112.
6. SUH, J., AND CHUNG, S. (1986) *Korean Biochem. J* **19,** 275.
7. SANDER, M. E., AND WITZEL, H. (1985) *Biochem. Biophys. Res. Commun.* **132,** 681.
8. SANDER, M. E., AND WITZEL, H. (1986) *in* Zinc Enzymes (Bertini, I., Luchinat, C., Maret, W., and Zeppezauer, M., Eds.), Chap. 13, Birkhauser, Boston.
9. TOMALIN, G., KAISER, B. L., KAISER, E. T. (1970) *J. Amer. Chem. Soc.* **92,** 6046.
10. HOFFMAN, S. J., CHU, S. S.-T., LEE, H.-H., KAISER, E. T., AND CAREY, P. R. (1983) *J. Amer. Chem. Soc.* **105,** 6971.
11. HILVERT, D., GARDELL, S. J., RUTTER, W. J., AND KAISER, E. T. (1986) *J. Amer. Chem. Soc.* **108,** 5298.
12. BRESLOW, R., AND WERNICK, D. L. (1976) *J. Amer. Chem. Soc.* **98,** 259.
13. BRESLOW, R., AND WERNICK, D. L. (1977) *Proc. Natl. Acad. Sci. USA* **74,** 1303.
14. GALDES, A., AULD, D. S., AND VALLEE, B. L. (1983) *Biochemistry* **22,** 1888.
15. GEOGHEGAN, K. F., GALDES, A., MARTINELLI, R. A., HOLMQUIST, B., AULD, D. S., AND VALLEE, B. L. (1983) *Biochemistry* **22,** 2255.
16. MAKINEN, M. W., YAMAMURA, K., AND KAISER, E. T. (1976) *Proc. Natl. Acad. Sci. USA* **73,** 3882.
17. KUO, L. C., AND MAKINEN, M. W. (1985) *J. Amer. Chem. Soc.* **107,** 5255.
18. CHRISTIANSON, D. W., AND LIPSCOMB, W. N. (1986) *J. Amer. Chem. Soc.* **108,** 4998.
19. KUO, L. C., LIPSCOMB, W. N., AND MAKINEN, M. W. (1986) *J. Amer. Chem. Soc.* **108,** 5003.
20. JONES, R. A. Y. (1984) Physical and Mechanistic Organic Chemistry, 2nd ed., p. 9, Cambridge Univ. Press, Cambridge.
21. WORTHING, A. G., AND GEFFNER, J. (1960) Treatment of Experimental Data, Chap. 9, Wiley, New York.
22. SCHEPARTZ, A., AND BRESLOW, R. (1987) *J. Amer. Chem. Soc.* **109,** 1814.
23. HAMMETT, L. P. (1970) Physical Organic Chemistry, 2nd ed., pp. 73–75, McGraw–Hill, New York.